

# Solid-State Magic-Angle Spinning NMR of Outer-Membrane Protein G from *Escherichia coli*

Matthias Hiller,<sup>[a]</sup> Ludwig Krabben,<sup>[a]</sup> Kutti R. Vinothkumar,<sup>[b]</sup> Federica Castellani,<sup>[a]</sup> Barth-Jan van Rossum,<sup>[a]</sup> Werner Kühlbrandt,<sup>[b]</sup> and Hartmut Oschkinat\*<sup>[a]</sup>

Uniformly <sup>13</sup>C-, <sup>15</sup>N-labelled outer-membrane protein G (OmpG) from *Escherichia coli* was expressed for structural studies by solid-state magic-angle spinning (MAS) NMR. Inclusion bodies of the recombinant, labelled protein were purified under denaturing conditions and refolded in detergent. OmpG was reconstituted into lipid bilayers and several milligrams of two-dimensional crys-

tals were obtained. Solid-state MAS NMR spectra showed signals with an apparent line width of 80–120 Hz (including homonuclear scalar couplings). Signal patterns for several amino acids, including threonines, prolines and serines were resolved and identified in 2D proton-driven spin-diffusion (PDS) spectra.

## Introduction

Structural investigations of membrane proteins at high resolution have proven to be difficult, primarily because well-ordered 3D crystals do not form easily and many of them cannot be solubilised in a manner suitable for solution NMR. Over the past few years, solid-state NMR has developed into a complementary method for structural research.<sup>[1–7]</sup> An important prerequisite for solid-state NMR is the availability of isotopically <sup>15</sup>N- and/or <sup>13</sup>C-labelled, preferably ordered, protein samples. In this paper, we describe the preparation of isotopically labelled 2D crystals of the outer-membrane protein G (OmpG) suitable for structural studies by solid-state MAS NMR.

The outer membrane of Gram-negative bacteria serves as a semipermeable barrier for small molecules. *Escherichia coli* contains a set of outer-membrane proteins, the so-called porins, that form channels allowing the influx of nutrients.<sup>[8,9]</sup> The porin OmpG is expressed in *E. coli* mutants lacking OmpF and LamB.<sup>[10]</sup> Thus, OmpG facilitates the growth of these porin-deficient mutants on maltodextrin-containing media. The gene for OmpG encodes a 301 amino acid (aa) polypeptide that is processed during export; this results in the removal of a 21 aa leader sequence to yield the mature protein. OmpG has the typical attributes of a bacterial porin: i) CD-spectroscopy indicates the presence of  $\beta$ -structure,<sup>[11]</sup> ii) the last residue is phenylalanine, which plays an important role in the insertion of the protein into the outer membrane;<sup>[12]</sup> iii) OmpG acts as a nonselective channel for mono-, di- and trisaccharides, as was shown by a proteoliposome swelling assay.<sup>[11]</sup>

In contrast to the well-known trimeric porins (e.g. OmpF, OmpC, PhoE and LamB), OmpG appears to be monomeric, since oligomeric forms were not detected on gels before or after chemical cross-linking.<sup>[11]</sup> Furthermore, in vitro-refolded OmpG is functional as a monomer in planar bilayers.<sup>[13]</sup> A projection structure at 6 Å resolution obtained by electron cryo-microscopy of 2D crystals shows a monomeric channel restricted by internal loops.<sup>[14]</sup> The inner diameter of the barrel is ~25 Å; this suggests that OmpG may have 14 membrane-

spanning  $\beta$ -strands. To determine the exact molecular architecture and to understand the size selectivity of this unique porin, detailed information on its 3D structure is needed.

An important consideration for structural studies by solid-state MAS NMR is the strategy for sample preparation.<sup>[15–17]</sup> Conformational disorder as a result of lyophilisation leads to substantial line broadening. Short-range local order in the sample is therefore desirable to obtain sufficient resolution. One way to achieve this is to prepare small microcrystals. Highly resolved solid-state MAS NMR spectra have thus been obtained from microcrystals (100–1000 nm diameter) of the  $\alpha$ -spectrin SH3 domain<sup>[15]</sup> and of nanocrystalline protein precipitates (10–100 nm diameter).<sup>[16]</sup> The resolution of spectra from micro- and nanocrystalline protein preparations was found to be similar; this demonstrates that crystalline aggregates in the 10 nm to 100 nm range are “large” enough to yield excellent resolution.<sup>[16]</sup> This was supported by studies on the bovine pancreatic trypsin inhibitor (BPTI), a chemotactic peptide, and the regulatory protein Crh.<sup>[18–20]</sup>

However, few solid-state MAS NMR studies of fully labelled, integral membrane proteins have been documented. One example is the solid-state MAS NMR investigation of the LH2 light-harvesting complex from *Rhodospseudomonas acidophila*,<sup>[21,22]</sup> which yielded assignments of the <sup>15</sup>N, <sup>13</sup>C-signals for the membrane-spanning portion. The high resolution obtained for this sample is attributed to the intrinsic rotational symmetry of the homo-nonameric membrane protein complex. An impor-

[a] Dipl.-Ing. M. Hiller, Dr. L. Krabben, Dr. F. Castellani, Dr. B.-J. van Rossum, Prof. H. Oschkinat  
Forschungsinstitut für Molekulare Pharmakologie  
Robert-Rössle-Straße 10, 13125 Berlin (Germany)  
Fax: (+49) 30-9479-3169  
E-mail: oschkinat@fmp-berlin.de

[b] K. R. Vinothkumar, Prof. W. Kühlbrandt  
Department of Structural Biology, MPI of Biophysics  
Max-von-Laue Straße 3, 60438 Frankfurt am Main (Germany)

tant question that remains is to what extent does the degree of local order determine the resolution in solid-state MAS NMR spectra of membrane proteins.

## Results

### Protein expression, refolding and analysis

OmpG was expressed without the leader peptide but with an additional N-terminal methionine (starting with M-EERNDWH...) in *E. coli* BL21 (DE3), on M9 minimal medium with uniformly  $^{13}\text{C}$ -labelled glucose as the sole carbon source and  $^{15}\text{N}$ -labelled ammonium chloride as the sole nitrogen source. The protein was found in inclusion bodies, solubilised in urea (8 M) and purified under denaturing conditions to yield 25 mg protein per litre of culture. OmpG was refolded by dilution into a urea-free buffer containing *n*-dodecyl- $\beta$ -D-maltoside (DDM; 1 mM). Refolding was most efficient (>90%) at low protein concentrations (<50  $\mu\text{g mL}^{-1}$ ). The refolding process was monitored by SDS-PAGE,<sup>[13,23]</sup> which shows denatured OmpG migrating at an apparent molecular weight of 34 kDa (Figure 1 a, lane I), compared to 28 kDa for the refolded form (Figure 1 a, lane II). CD spectra of the preparation confirmed the efficient refolding of OmpG, showing a minimum at ~215 nm and a maximum at ~195 nm (Figure 1 b); this is typical of a  $\beta$ -sheet protein<sup>[11,13]</sup> and similar to results reported for native OmpG.<sup>[11]</sup> Single-channel activity of OmpG reconstituted into planar lipid bilayers resulted in a primary conductance of  $364 \pm 11$  pS (data not shown), comparable to data published earlier.<sup>[13]</sup>

### 2D crystallisation

After lowering the detergent concentration by a second anion-exchange-chromatography step, OmpG was reconstituted into lipid bilayers. 2D crystals were subsequently formed by dialysis. They were of tubular shape and measured up to 1  $\mu\text{m}$  in length and 130–180 nm in width (Figure 2a, inset). Electron micrographs of these crystals recorded by electron cryo-microscopy diffracted to ~8 Å. A projection map at 8 Å resolution (data not shown) indicated a circular shape essentially identical to that of the native porin.<sup>[14]</sup>

### 1D solid-state MAS NMR experiments

Figure 2a shows a 1D  $^{13}\text{C}$  cross-polarisation (CP)/MAS NMR spectrum of OmpG 2D crystals recorded at

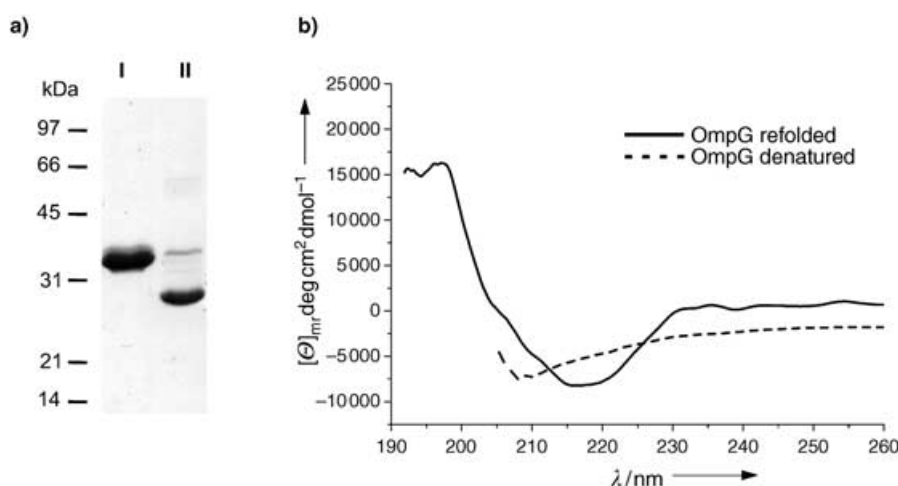


**Figure 1.** Expression, purification and refolding of OmpG. a) Lane I, purified OmpG under denaturing conditions (8 M urea and heating prior to sample application); lane II, refolded OmpG in 1 mM DDM without heating. b) Circular dichroism analysis of refolded and unfolded OmpG. The protein concentration was 25  $\mu\text{M}$ . Samples were scanned in a 1 mm path-length quartz cuvette, as described in the Experimental Section.

400 MHz. The spectrum exhibits carbonyl signals around 175 ppm, signals of aromatic carbons between 120 and 140 ppm and signals of aliphatic carbons occurring in the region from 10 to 80 ppm.

To verify that the sharp lines are indeed due to the short-range order present in the 2D crystals, we reconstituted OmpG into lipid vesicles. A 1D  $^{13}\text{C}$ -CP/MAS NMR spectrum of these vesicles, recorded under similar conditions to the spectrum in Figure 2a is depicted in Figure 2b. In this case, the strongest

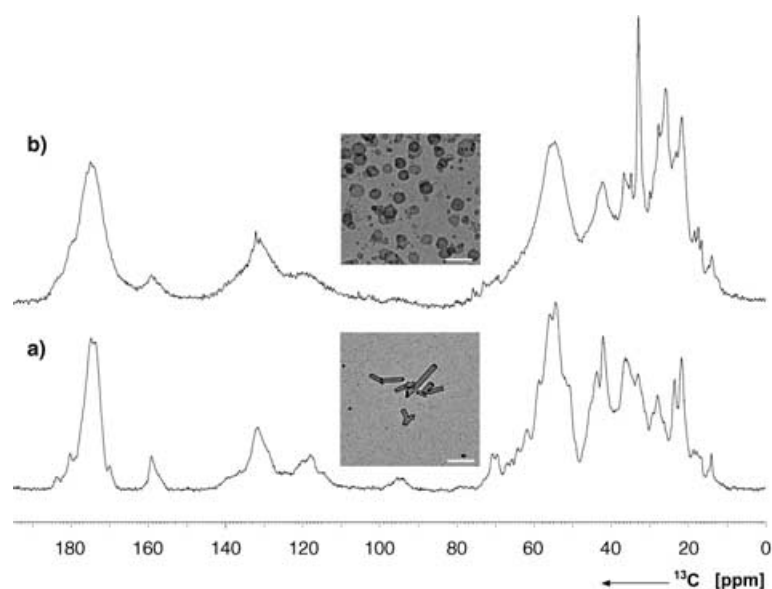


**Figure 2.** 1D  $^{13}\text{C}$ -CP/MAS NMR spectra of  $^{13}\text{C}$ ,  $^{15}\text{N}$ -labelled OmpG reconstituted into a) 2D crystals or b) lipid vesicles. The spectrum of the 2D crystals was recorded with 1024 scans. The NMR rotor contained 9 mg of protein and 4.5 mg lipids. The spectrum of the vesicles was recorded with 3072 scans on a sample containing 3 mg pure protein reconstituted in 4.5 mg *E. coli* lipids to achieve a comparable signal-to-noise ratio. The spectra were recorded at a spinning frequency of 8 kHz on a 400 MHz wide-bore spectrometer. Insets: Electron micrographs of vesicles (top) or 2D crystals (bottom) of OmpG; scale bars = 1  $\mu\text{m}$ .

and best-resolved signals are observed in the region from 10 to 40 ppm. These peaks are attributed to the  $^{13}\text{C}$  natural abundance background of the lipids. This was confirmed by comparison to spectra of pure lipid vesicles. The protein signals, however, appear much broader.

In a second series of 1D  $^{13}\text{C}$ -CP/MAS NMR experiments with OmpG crystals, we investigated the influence of temperature on spectral resolution. Measurements were performed at temperatures ranging from 240 to 280 K. Similar narrow lines were observed between 262 and 280 K. The resolution decreased when the sample was frozen and measured at 240 K (data not shown). These changes were reversible, and the higher resolution was fully recovered when the temperature was raised again to 280 K. Repeated freeze–thaw cycles had no effect on the resolution.

## 2D solid-state MAS NMR experiments

2D  $^{13}\text{C}$ – $^{13}\text{C}$  homonuclear correlation spectra of tubular OmpG 2D crystals were acquired by using the PDS technique.<sup>[24,25]</sup> Figure 3 shows a 2D correlation spectrum recorded with 20 ms mixing at 280 K. The strong diagonal signals arise from  $^{13}\text{C}$ -labelled sites in OmpG and from the  $^{13}\text{C}$  natural-abundance background of the lipids. The unlabelled lipids do not give rise to detectable cross peaks due to the low abundance of adjacent  $^{13}\text{C}$  nuclei. All observed cross peaks reflect intraresidual correlation networks of OmpG.<sup>[15,18,26,27]</sup> As an example, two threonine correlation patterns are shown in Figure 4a. We were able to identify signal sets for ten of the fifteen threonines in OmpG from complete correlation networks between

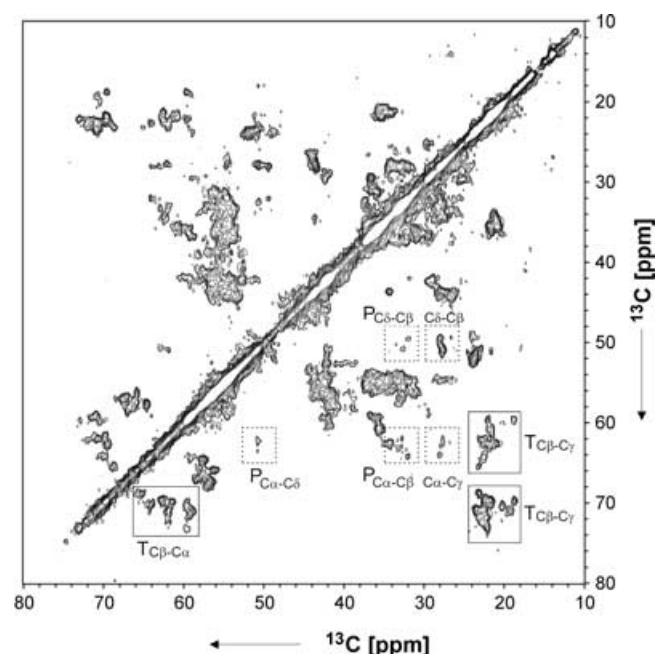


**Figure 3.** 2D  $^{13}\text{C}$ – $^{13}\text{C}$  PDS NMR spectrum of the OmpG 2D crystals. The spectrum was recorded at 600 MHz and 280 K with a mixing time of 20 ms and a MAS frequency of 9.5 kHz. The spectral area shown contains cross peaks for aliphatic carbons. The signal patterns for threonine (—) and proline (----) are indicated in boxes.

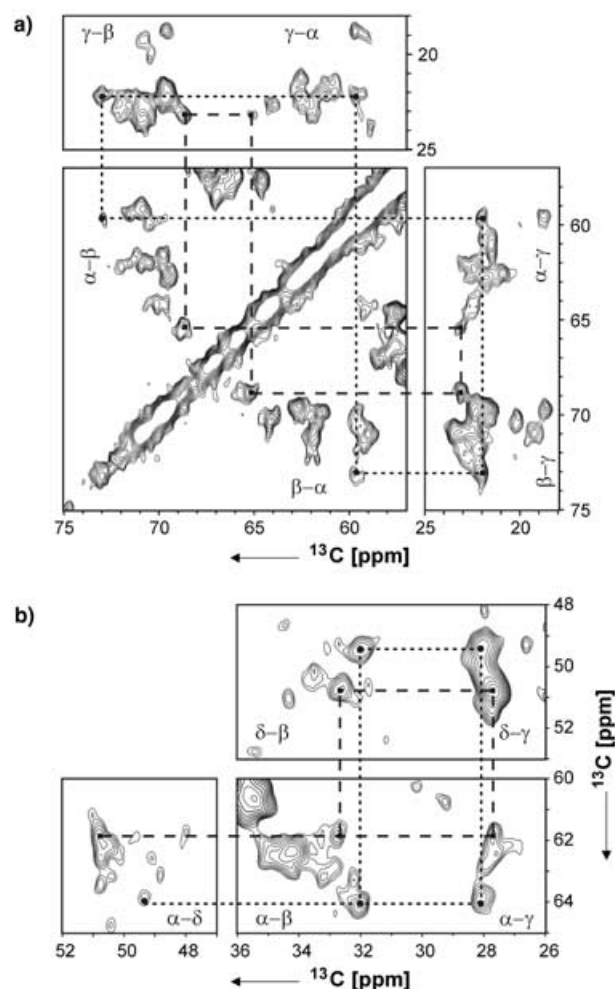


**Figure 4.** Threonine and proline signal patterns extracted from the 2D  $^{13}\text{C}$ – $^{13}\text{C}$  PDS NMR spectrum as shown in Figure 3. a) Complete correlation patterns involving  $\alpha$ ,  $\beta$  and  $\gamma$  carbons of two different threonine residues are connected by dashed or dotted lines. b) correlation patterns for the  $\alpha$ ,  $\beta$ ,  $\gamma$  and  $\delta$  carbons of two different proline residues are connected by dotted or dashed lines.

the  $\alpha$ ,  $\beta$  and  $\gamma$  carbons, which resonate between 58–66 ppm, 68–74 ppm and 18–24 ppm, respectively. In a similar way, we assigned six out of eight prolines due to their characteristic  $\alpha$ – $\beta$ ,  $\alpha$ – $\gamma$ ,  $\delta$ – $\beta$  and  $\delta$ – $\gamma$  correlations. For some of these we even detected  $\alpha$ – $\delta$  cross peaks (Figure 4b). Furthermore, we identified nine out of twelve serines. In spectra recorded with longer PDS mixing times (50–100 ms), several isoleucine patterns were found (not shown).

## Discussion

For structure determination of integral membrane proteins by solid-state MAS NMR, several conditions are critical: i) the availability of milligram amounts of protein, ii) incorporation of isotopes and iii) local order in the sample preparation used.

In this work, more than 12 mg of uniformly  $^{13}\text{C}$ -,  $^{15}\text{N}$ -labelled OmpG were prepared from a one litre culture by applying an efficient refolding protocol. The refolded protein (more than

90%) exhibited the same properties as the native form, as demonstrated by SDS-PAGE, CD-spectroscopy (Figure 1) and planar lipid-bilayer recordings. In addition, we generated 2D crystals that were well suited for solid-state MAS NMR (Figure 2a). This form of preparation has additional advantages, such as a high protein density and a low lipid-to-protein ratio (LPR). Furthermore, a quasinaive environment is generated since 2D crystals were formed from OmpG and an *E. coli* total lipids extract. However, the long-range order and translational symmetry, as required for diffraction techniques, is not important for solid-state NMR. The 2D crystals we used for NMR studies are unsuitable for high-resolution structure determination by cryo-EM, whereas well-resolved NMR spectra were readily obtained. In particular, 2D  $^{13}\text{C}$ - $^{13}\text{C}$  spectra show cross peaks with an apparent line width of 80–120 Hz (including scalar couplings; Figures 3 and 4). This resolution is sufficient for the identification of a large number of amino acid signal patterns (e.g. Figure 4).

Spectra obtained from vesicles, however, show less resolved lines. These broader lines are due to the less-defined environment of each protein molecule. This is evident from Figure 2, in which 1D spectra of OmpG in 2D crystals (a) and in noncrystalline vesicles (b) are compared. Another disadvantage of the vesicle preparation is that it contains less protein per volume than the 2D crystals. Since the sample volume of the NMR container is limited, this results in lower signal intensities.

To understand the observed strong effect of short-range order on spectral resolution, it should be realised that OmpG is a transmembrane  $\beta$ -barrel rather than a globular protein. Experience shows that buried residues of membrane proteins and receptor-bound agonists or antagonists give rise to sharp lines.<sup>[5,28]</sup> In these cases, the signals are from nuclei in a conformationally homogeneous environment that determines the resolution. Since OmpG is a transmembrane  $\beta$ -barrel, it lacks a well-defined hydrophobic core, and most residues are located in a single-walled cylindrical  $\beta$ -sheet, facing either the lipid bilayer or the solvent in the pore. In this way, most residues are surface-exposed. It appears that 2D crystallisation locks these residues in one conformation and thus might have a stronger effect on the spectral resolution than for other membrane proteins.

NMR spectra recorded below the freezing point of the sample exhibit line broadening. This might indicate a disruption of the 2D crystal lattice by mechanical stress due to the formation of ice crystals. However, the resolution is recovered after increasing the sample temperature to 280 K. Our observation that the resolution changes reversibly and recovers directly after thawing makes it unlikely that the 2D crystals are destroyed. Alternatively, the observed line broadening might be due to the reduced mobility of side-chains in the frozen state, resulting in reduced self-decoupling. However, increasing the decoupling power from 70 to 110 kHz had no effect on the 1D spectra of a frozen sample of OmpG 2D crystals (data not shown). This increase would normally be sufficient to induce heteronuclear decoupling in a rigid body. The most likely explanation for this effect is the structural inhomogeneity of side chains immobilised by frozen water and a more rigid lipid

phase. This is in line with recent reports by Martin et al.,<sup>[16]</sup> who show that sample freezing causes incomplete motional averaging and results in in-homogeneous line broadening. Noteworthy is that 2D crystals show spectra with narrow lines at room temperature, in contrast to micellar solutions, which require freezing.<sup>[22]</sup>

Despite the favourable line width, resonance overlap hampers the specific assignment of resonances in crowded regions. A significant improvement is possible by incorporating fewer  $^{13}\text{C}$  atoms in defined positions in the protein. This can be achieved by growing the bacteria on a medium containing either 1,3- $^{13}\text{C}$ - or 2- $^{13}\text{C}$ -glycerol as the sole carbon source.<sup>[29–32]</sup> The effect of this reduced labelling on the quality of the spectra is twofold: it simplifies the spectra and removes most of the broadening due to  $J$  couplings. In addition, this kind of spin dilution allows the detection of the necessary long-range correlations for structure calculations. This work is currently in progress.

In conclusion, the results presented here demonstrate that small, poorly ordered 2D crystals of an integral membrane protein are suitable for structure determination by solid-state MAS NMR. We expect that this approach is generally suitable for structural studies of membrane proteins and their complexes.

## Experimental Section

**Chemicals:** Chemicals were purchased from the following suppliers: OG and DDM from Glycon, Luckenwalde, Germany; *E. coli* total-lipid extract from Avanti Polar Lipids, Alabaster, USA; Q-Sepharose Fast Flow and Resource-Q columns from Amersham Biosciences, Freiburg, Germany. All other reagents were purchased from VWR International, Darmstadt, Germany, at the highest purity available.

**Cloning and strains:** The coding sequence for OmpG was amplified from chromosomal DNA (D2001) of *E. coli* strain B (SIGMA, Deisenhofen, Germany) by using the following primers: forward, 5'-GATCTCGGTTGGGCTGGCTTCTGTCTCCCT; reverse, 5'-CCGACG-CAGGAGTTAGGTCAACAAAGCTGCG. The product was used in a second PCR (primers: forward, 5'-GGCCTGCGACATATGGAAGAAAGGAAAGCGAC; reverse 5'-CGGATAAGGAGCTCGCGCGCATCC) to introduce the restriction sites *NdeI* and *SacI*. The amplified DNA was digested with *NdeI* and *SacI* and cloned into a pET-26b expression plasmid from Novagen (Bad Soden, Germany). The resulting construct contained the mature form of OmpG (280 amino acids) without signal sequence, plus an N-terminal methionine. Protein expression was carried out in *E. coli* BL21 (DE3) cells from Novagen (Bad Soden, Germany).

**Expression and purification of  $^{13}\text{C}$ -,  $^{15}\text{N}$ -labelled OmpG:** An overnight culture was diluted to an  $\text{OD}_{600}$  of 0.1 in M9 minimal media. For fully  $^{13}\text{C}$ -,  $^{15}\text{N}$ -labelled OmpG, uniformly  $^{13}\text{C}$ -labelled glucose ( $2\text{ g L}^{-1}$  culture) and  $^{15}\text{N}$ -ammonium chloride ( $0.5\text{ g L}^{-1}$  culture) were used as the sole carbon and sole nitrogen sources, respectively. At an  $\text{OD}_{600}$  of 0.6–0.7, the expression of OmpG was induced by isopropyl- $\beta$ -D-thiogalactopyranoside (1 mM). Cells were further incubated for 3 h at 37°C and collected by centrifugation at 5000g for 15 min at 4°C. The pellet was washed with ice-cold NaCl solution (500 mL, 0.15 M), centrifuged and frozen. Protein purification was carried out in a similar manner to that described by Conlan et al.<sup>[13]</sup> In brief, cells from a 1 L culture were broken by



using a French Press. The solubilised inclusion body fraction was loaded on to a Q-Sepharose Fast-Flow column with a bed volume of 180 mL. The column was washed with three column volumes of buffer A (10 mM Tris-HCl, pH 8.0) containing urea (8 M). OmpG was eluted with a linear gradient of NaCl (0–1 M). The concentration of OmpG was determined by measuring the absorbance at 280 nm in buffer A containing urea (8 M) with an extinction coefficient of  $85\,060\text{ M}^{-1}\text{ cm}^{-1}$ .<sup>[33]</sup>

**Refolding and 2D crystallisation:** For refolding, purified OmpG was diluted into buffer A containing DDM (1 mM) and L-arginine (0.6 M) at 8°C by using a peristaltic pump with a flow rate of 0.1 mL min<sup>-1</sup>. The refolded protein was washed and concentrated with buffer A and DDM (1 mM) to a final concentration of 1–2 mg mL<sup>-1</sup> in an ultrafiltration chamber (Millipore, Schwalbach, Germany) with a membrane cut-off of 30 kDa. The detergent concentration was reduced by binding OmpG to a Resource-Q column and washing with 3 column volumes of buffer A with DDM (0.4 mM). OmpG was eluted with NaCl (0.3 M) and concentrated by a centrifugal filter device (Ultrafree-15, cut-off 50 kDa, Millipore; final concentration 3 mg mL<sup>-1</sup>). Refolded OmpG was reconstituted into lipid bilayers. For this purpose, an *E. coli* total lipid chloroform extract (20 mg) was dried in a nitrogen stream. The resulting lipid film was dissolved in buffer A (5 mL) containing OG (34 mM). Aliquots of this lipid solution and refolded OmpG (2 mg mL<sup>-1</sup>) were mixed to yield a lipid-to-protein ratio (LPR) of 1:2 (w/w). For 2D crystallisation, the detergent was removed by dialysis (dialysis-tube cut-off 25 kDa, Roth, Karlsruhe, Germany) at 20°C against buffer B (5 L, 20 mM Tris-HCl, pH 7.0, 25 mM MgCl<sub>2</sub>, 3 mM NaN<sub>3</sub>, 150 mM NaCl) for 6 to 7 weeks. The dialysis buffer was changed every 5 days. 2D crystals were observed after 7 days. OmpG reconstituted into lipid vesicles was prepared in the same way, except that the LPR was adjusted to 3:2, and dialysis was stopped after 7 days.

**Circular dichroism spectroscopy:** CD spectra were taken on a J720 CD-spectrometer from Jasco (Tokyo, Japan) in a quartz cuvette with 1 mm path length. Unfolded and folded protein (25 μM) was measured in buffer A containing urea (8 M) or DDM (0.4 mM), respectively. Each sample was scanned 5 times from 260 to 190 nm with a step size of 1 nm. Data were baseline corrected and converted to molar residue ellipticity.

**Electron microscopy:** The crystallised samples (2–4 μL) were applied to a carbon-coated grid (400 mesh copper rhodium) from PLANO (Wetzlar, Germany) and incubated for 20 s. The grid was stained twice with drops (2 μL) of uranyl acetate solution (2%, w/v). Residual liquid was removed after each step. Images were recorded on a CM12 electron microscope (Philips) at an accelerating voltage of 120 kV with an electron dose of  $10\text{ e}^{-}\text{Å}^{-2}$  on Kodak SO-163 film at 60 000× magnification.

**Planar lipid-bilayer recordings:** Planar lipid bilayers were prepared as described previously.<sup>[34]</sup> OmpG was added to one measurement chamber (final concentration 30 ng mL<sup>-1</sup>) in buffer A with NaCl (0.3 M). The transmembrane current was measured under voltage-clamp conditions by using a routine patch-clamp amplifier (model EPC9, HEKA, Germany). To monitor the ion current, the sampling frequency of the patch-clamp amplifier was fixed at 0.5 kHz, with a 4-pole Bessel filter and a 3-dB corner frequency of 0.1 kHz. The raw data were analysed with the TAC software package (Bruyton Corporation, Seattle, WA). Gaussian filters between 7 and 37 kHz were applied to reduce noise.

**Solid-state MAS NMR spectroscopy:** 2D crystals of OmpG were sedimented in an ultracentrifuge at 100 000g for 30 min and 4°C in phosphate buffer (20 mM) with NaCl (50 mM). Samples were

transferred into a 4 mm MAS rotor (Bruker, Karlsruhe, Germany) by centrifugation at 19 000g for 10 min. NMR measurements were performed on DMX-600 and DMX-400 spectrometers (Bruker), both equipped with a 4 mm triple-resonance MAS probe (Bruker).

One-dimensional <sup>13</sup>C CP/MAS NMR spectra were recorded on a 400 MHz wide-bore spectrometer at different temperatures (280–240 K) and at a MAS frequency  $\omega_R/2\pi$  of 8.0 kHz. Magnetisation was transferred from <sup>1</sup>H to <sup>13</sup>C with a ramped CP contact of 500 μs. For decoupling, the two-pulse phase modulation (TPPM)<sup>[35]</sup> with a pulse width of 6–7.5 μs and a proton RF field of ~70 kHz was used. All 1D spectra were recorded with the same acquisition time (40 ms).

2D <sup>13</sup>C–<sup>13</sup>C spectra of OmpG were recorded at a magnetic field strength of 14.1 T at 280 K with a MAS frequency  $\omega_R/2\pi$  of 9.5 kHz by using the proton-driven spin-diffusion (PDS) mixing scheme.<sup>[36]</sup> Magnetisation was transferred from <sup>1</sup>H to <sup>13</sup>C with a ramped CP of 1.75 ms and spinlock field strengths of ~60 kHz for <sup>1</sup>H and 45–90 kHz for the <sup>13</sup>C ramp. A PDS mixing time of 20 ms was chosen, and a proton RF field of ~70 kHz was applied for TPPM decoupling. 96 scans per increment were collected, with an effective evolution time of ~7.7 ms in the indirect dimension. The 2D data were thus recorded in 2 days. Data were processed by using XWINNMR, version 2.6 (Bruker, Karlsruhe, Germany) and subsequently analysed in Sparky, version 3.1 (T. D. Goddard, D. G. Kneller, University of California, USA).

## Abbreviations

CP, cross polarisation; DDM, *n*-dodecyl-β-D-maltoside; LPR, lipid-to-protein ratio; MAS, magic angle spinning; OG, *n*-octyl-β-D-glucopyranoside; OmpG, outer-membrane protein G; PDS, proton-driven spin-diffusion; RF, radio frequency; TPPM, two-pulse phase-modulation.

## Acknowledgements

This work was supported by a grant from the BMBF (ProAMP). We thank Dr. Anne Diehl for helpful discussions, and Prof. Dr. P. Pohl and Dr. S. Saporov for the planar lipid-bilayer recordings.

**Keywords:** membrane proteins · protein folding · solid-state NMR · structure elucidation

- [1] T. A. Cross, *Methods Enzymol.* **1997**, *289*, 672–696.
- [2] R. G. Griffin, *Nat. Struct. Biol. NMR Suppl.* **1998**, *7*, 508–512.
- [3] H. J. M. de Groot, *Curr. Opin. Struct. Biol.* **2000**, *10*, 593–600.
- [4] L. K. Thompson, *Curr. Opin. Struct. Biol.* **2002**, *12*, 661–669.
- [5] A. Watts, *Mol. Membr. Biol.* **2002**, *19*, 267–275.
- [6] S. Luca, H. Heise, M. Baldus, *Acc. Chem. Res.* **2003**, *36*, 858–865.
- [7] S. J. Opella, F. M. Marassi, *Chem. Rev.* **2004**, *104*, 3587–3606.
- [8] H. Nikaïdo, *J. Bacteriol.* **1999**, *181*, 4–8.
- [9] H. Nikaïdo, *Microbiol. Mol. Biol. Rev.* **2003**, *67*, 593–623.
- [10] R. Misra, S. A. Benson, *J. Bacteriol.* **1989**, *171*, 4105–4111.
- [11] D. A. Fajardo, J. Cheung, C. Ito, E. Sugawara, H. Nikaïdo, R. Misra, *J. Bacteriol.* **1998**, *180*, 4452–4459.
- [12] M. Struyve, M. Moons, J. Tommassen, *J. Mol. Biol.* **1991**, *218*, 141–148.
- [13] S. Conlan, Y. Zhang, S. Cheley, H. Bayley, *Biochemistry* **2000**, *39*, 11 845–11 854.
- [14] M. Behlau, D. J. Mills, H. Quader, W. Kühlbrandt, J. Vonck, *J. Mol. Biol.* **2001**, *305*, 71–77.
- [15] J. Pauli, B. van Rossum, H. Förster, H. J. M. de Groot, H. Oschkinat, *J. Magn. Reson.* **2000**, *143*, 411–416.

- [16] R. W. Martin, K. W. Zilm, *J. Magn. Reson.* **2003**, *165*, 162–174.
- [17] S. K. Straus, *Philos. Trans. R. Soc. London Ser. B* **2004**, *359*, 997–1008.
- [18] A. McDermott, T. Polenova, A. Bockmann, K. W. Zilm, E. K. Paulson, R. W. Martin, G. T. Montelione, E. K. Paulsen, *J. Biomol. NMR* **2000**, *16*, 209–219.
- [19] C. M. Rienstra, L. Tucker-Kellogg, C. P. Jaroniec, M. Hohwy, B. Reif, M. T. McMahon, B. Tidor, T. Lozano-Perez, R. G. Griffin, *Proc. Natl. Acad. Sci. USA* **2002**, *99*, 10260–10265.
- [20] A. Böckmann, A. Lange, A. Galinier, S. Luca, N. Giraud, M. Juy, H. Heise, R. Montserret, F. Penin, M. Baldus, *J. Biomol. NMR* **2003**, *27*, 323–339.
- [21] T. A. Egorova-Zachernyuk, J. Hollander, N. Fraser, P. Gast, A. J. Hoff, R. Cogdell, H. J. M. de Groot, M. Baldus, *J. Biomol. NMR* **2001**, *19*, 243–253.
- [22] A. J. van Gammeren, F. B. Hulsbergen, J. G. Hollander, H. J. M. de Groot, *J. Biomol. NMR* **2004**, *30*, 267–274.
- [23] M. G. Beher, C. A. Schnaitman, A. P. Pugsley, *J. Bacteriol.* **1980**, *143*, 906–913.
- [24] N. Bloembergen, *Physica* **1949**, *15*, 386–426.
- [25] D. Suter, R. R. Ernst, *Phys. Rev. B* **1985**, *32*, 5608–5627.
- [26] S. K. Straus, T. Bremi, R. R. Ernst, *J. Biomol. NMR* **1997**, *10*, 119–128.
- [27] J. Pauli, M. Baldus, B. van Rossum, H. de Groot, H. Oschkinat, *ChemBioChem* **2001**, *2*, 272–281.
- [28] L. Krabben, B. J. van Rossum, F. Castellani, E. Bocharov, A. A. Schulga, A. S. Arseniev, C. Weise, F. Hucho, H. Oschkinat, *FEBS Lett.* **2004**, *564*, 319–324.
- [29] D. M. LeMaster, D. M. Kushlan, *J. Am. Chem. Soc.* **1996**, *118*, 9255–9264.
- [30] M. Hong, *J. Magn. Reson.* **1999**, *139*, 389–401.
- [31] F. Castellani, B. van Rossum, A. Diehl, M. Schubert, K. Rehbein, H. Oschkinat, *Nature* **2002**, *420*, 98–102.
- [32] F. Castellani, B. J. van Rossum, A. Diehl, K. Rehbein, H. Oschkinat, *Biochemistry* **2003**, *42*, 11476–11483.
- [33] S. C. Gill, P. H. von Hippel, *Anal. Biochem.* **1989**, *182*, 319–326.
- [34] P. Pohl, S. M. Saparov, *Biophys. J.* **2000**, *78*, 2426–2434.
- [35] A. E. Bennett, C. M. Rienstra, M. Auger, K. V. Lakshmi, R. G. Griffin, *J. Chem. Phys.* **1995**, *103*, 6951–6958.
- [36] N. M. Szeverenyi, M. J. Sullivan, G. E. Maciel, *J. Magn. Reson.* **1982**, *47*, 462–475.

---

Received: March 31, 2005